JIPB Journal of Integrative Plant Biology

Maize ZmVPP5 is a truncated Vacuole H^+-PPase that confers hypersensitivity to salt stress

Xiaoliang Sun[1], Weiwei Qi[1,2], Yihong Yue[1], Huiling Ling[1], Gang Wang[1,2] and Rentao Song[1,2]*

[1]Shanghai key Laboratory of Bio-Energy Crops, School of Life Sciences, Shanghai University, Shanghai 200444, China, [2]Coordinated Crop Biology Research Center(CBRC), Beijing 100193, China. *Correspondence: rentaosong@staff.shu.edu.cn

Abstract In plants, Vacuole H^+-PPases (VPPs) are important proton pumps and encoded by multiple genes. In addition to full-length VPPs, several truncated forms are expressed, but their biological functions are unknown. In this study, we functionally characterized maize vacuole H^+-PPase 5 (*ZmVPP5*), a truncated VPP in the maize genome. Although ZmVPP5 shares high sequence similarity with ZmVPP1, ZmVPP5 lacks the complete structure of the conserved proton transport and the inorganic pyrophosphatase-related domain. Phylogenetic analysis suggests that *ZmVPP5* might be derived from an incomplete gene duplication event. *ZmVPP5* is expressed in multiple tissues, and ZmVPP5 was detected in the plasma membrane, vacuole membrane and nuclei of maize cells. The overexpression of *ZmVPP5* in yeast cells caused a hypersensitivity to salt stress. Transgenic maize lines with overexpressed *ZmVPP5* also exhibited the salt hypersensitivity phenotype. A yeast two-hybrid analysis identified the ZmBag6-like protein as a putative ZmVPP5-interacting protein. The results of bimolecular luminescence complementation (BiLC) assay suggest an interaction between ZmBag6-like protein and ZmVPP5 *in vivo*. Overall, this study suggests that ZmVPP5 might act as a VPP antagonist and participate in the cellular response to salt stress. Our study of ZmVPP5 has expanded the understanding of the origin and functions of truncated forms of plant VPPs.

Keywords: Maize; salt stress; vacuole H^+-PPases; ZmBag6-like protein; ZmVPP5
Citation: Sun X, Qi W, Yue Y, Ling H, Wang G, Song R (2016) Maize ZmVPP5 is a truncated Vacuole H^+-PPase that confers hypersensitivity to salt stress. **J Integr Plant Biol** XX:XX–XX doi: 10.1111/jipb.12462
Edited by: Jianqiang Wu, Kunming Institute of Botany, CAS, China
Received Nov. 12, 2015; **Accepted** Dec. 31, 2015
Available online on Jan. 5, 2016 at www.wileyonlinelibrary.com/journal/jipb

Research Article

OnlineOpen

INTRODUCTION

In plant cells, vacuoles are multifunctional organelles involved in cell growth, storage, and detoxification (Viotti et al. 2013). Based on the different functions, plant vacuoles are classified as lytic vacuoles (LVs) or protein storage vacuoles (PSVs) (Jiang et al. 2000). The plant vacuoles are the major storage organelles for metabolites and nutrients and play an important role in maintaining osmotic pressure (Zhou et al. 2014). The maintenance of the morphology and function of vacuoles is critical for cell function.

Proton pumps are important for vacuolar morphology and functions. There are two types of vacuolar proton pumps, H^+-ATPase (V-ATPase) and H^+-pyrophosphatase (V-PPase). Both pumps participate in establishing a proton motive force across the tonoplast to drive the secondary transport of sucrose, organic acids and secondary metabolites into vacuoles (Seidel et al. 2013). Although V-PPase activity functionally complements V-ATPase activity (Perez-Castineira et al. 2011), their activities and abundance are differentially regulated in response to environmental stress (Dell'orto et al. 2013; van Schalkwyk et al. 2013; Anjaneyulu et al. 2014). Our understanding of plant V-ATPases has been greatly advanced in recent years; however, many questions remain unanswered regarding V-PPases, such as the number of V-PPase isoforms and the differences in their functions (Gaxiola et al. 2007).

V-PPases play a role in growth and development (Mohammed et al. 2012). In addition to vacuolar acidification, V-PPase can increase plant biomass, cell division at the onset of organ formation, auxin transport and stress resistance (Gaxiola et al. 1999; Li et al. 2005; Gaxiola et al. 2007). In the model plant *Arabidopsis*, VPPs contain two isoforms, i.e., AVP1 and AVP2. AVP1 and AVP2 coexist in the plant cell and catalyze PPi hydrolysis and H^+ translocation. However, the isoforms have divergent primary structures that lead to different subcellular localizations, and they differ in their metal requirements and sensitivities (Mitsuda et al. 2001; Gaxiola et al. 2007). Sequence analysis shows that the VPP family has a high degree of sequence homology (81%–91%). However, the number of VPP isoforms differs in some plant species. For example, tobacco has three isoforms, and rice has five isoforms (Gaxiola et al. 2007). These different isoforms may be differentially regulated in plants (Maeshima 2000). Therefore, their evolutionary relationships and functions deserve further analysis.

In this study, we identified 12 expressed VPP genes in the maize genome based on sequence analyses. Among these genes are two truncated VPPs with unknown function. We further characterized one of the truncated VPP members, *ZmVPP5*, which might derive from full-length type I VPPs.

ZmVPP5 is expressed in multiple tissues, and the protein is located on the plasma membrane, vacuole membrane, and nuclei. Overexpressing *ZmVPP5* in maize and yeast cells conferred hypersensitivity to salt stress. Through yeast two-hybrid screening, we also identified a ZmBag6-like protein as a ZmVPP5 interacting protein; co-localization and BiLC assays supported their interaction *in vivo*. This study of ZmVPP5 expanded our understanding of the origin and functions of the truncated form of VPPs in plants.

RESULTS

ZmVPP5 is a truncated and expressed member of the VPP family

To obtain all members of the VPP family in maize (*zea mays*), BLAST analysis was performed using the sequence of maize VPP1 FL-cDNA against the maize cDNA database and genome database. Nineteen homologous members were identified; however, seven of them did not have transcripts in any tissue according to expressed sequence tag (EST) information (http://www.maizegdb.org/). Sequence alignment analysis indicated that *ZmVPPs* can be divided into five subgroups based on their putative transmembrane (TM) domain numbers (Figure 1A) and sequence divergence (Figure 1B). For example, Type I VPPs are VPP1-like proteins that contain 15 TMs. Type IV and Type V VPPs are both truncated VPP proteins containing 3–5 TMs. Type IV and Type V VPPs both have a signal peptide predicted online (http://www.cbs.dtu.dk/services/SignalP/) which might take part in the transformation of proteins into the endoplasmic reticulum (ER) lumen. And this signal peptide is absent in the full-length VPPs.

We cloned *ZmVPP5* cDNA using gene-specific primers designed according to NP_001140455. The presence of *ZmVPP5* in the cDNA indicated that *ZmVPP5* is a transcribed gene. We raised a ZmVPP5 specific antibody to a C-terminal specific polypeptide "VSGVQPSFSLNRKEL" from ZmVPP5, and the ZmVPP5-specific antibody could detect ZmVPP5, showing an expected molecular mass of 18.7 kDa (Figure 1C). The result indicated that ZmVPP5 protein is translated in maize.

Phylogenetic analysis of VPPs proteins

To understand the evolutionary relationship of truncated VPPs, e.g., *ZmVPP5*, to other VPPs, a phylogenetic tree was constructed. Typical VPPs have a molecular weight of 71–80 kDa with 14–17 transmembrane helices (TMs) (Maeshima

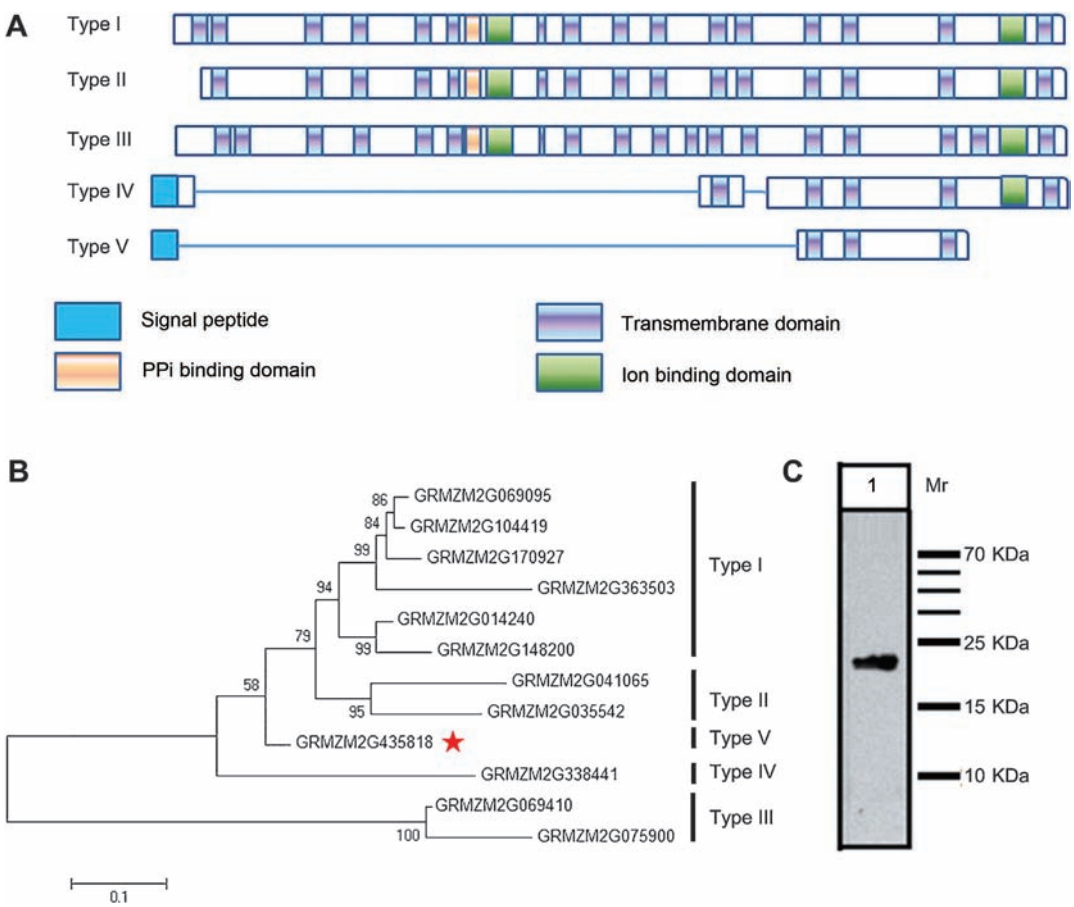

Figure 1. ZmVPP5 is a truncated vacuole H^+-PPases (VPPs) protein

(A) The *Zea mays* VPPs family contains five types according to the number of transmembrane (TM) motifs. **(B)** Phylogenetic tree for the VPPs family based on the VPP protein sequence of *Zea mays*. Asterisk indicates ZmVPP5. The scale 0.1 is the genetic distance. **(C)** Western-blot analysis of ZmVPP5.

2000). However, truncated VPP proteins were also found in some plants, such as *Arabidopsis* (gi|62321314, 173 amino acids (aa)), *grape* (gi|6319128, 167 aa), *Oryza sativa* (gi|125538363, 288 aa) and *Dimocarpus longan* (gi|338172901, 163 aa). Based on the phylogenetic analysis, these truncated VPP proteins did not form a separate clade among the different species (Figure S1). The results indicated that each truncated VPPs member has an independent origin and that they probably derived from full-length VPPs during gene duplication events.

ZmVPP5 is expressed in multiple tissues

The analysis of expression data (http://www.maizeGDB.org) for *ZmVPP5* (GRMZM2G435818) revealed that the *ZmVPP5* gene is expressed in multiple tissues.

The *ZmVPP5* expression was further examined using quantitative real-time polymerase chain reaction (qRT-PCR) and western-blot. The transcript level of *ZmVPP5* is high in the silk, husk and tassel and in the early stage of kernel development but is low in the leaves, root and in the mid stage of kernel development (Figure 2). The ZmVPP5 protein was detected in the stem, husk, silk, tassel and kernel. The RNA and protein levels of ZmVPP5 were highly correlated.

ZmVPP5 is localized to the plasma membrane, vacuolar membrane, and nuclei

To determine the subcellular localization of the ZmVPP5 protein, YFP-ZmVPP5 fusion protein was constructed. The predicted localization of ZmVPP5 is the plasma membrane (http://wolfpsort.org/). Co-localization with different organelle localization markers indicated that ZmVPP5 localizes to the plasma membrane, vacuolar membrane and nuclei (Figure S2).

Subcellular fractionation was further used to analyze the presence of ZmVPP5 in different subcellular fractions. The total protein was extracted from maize tassel and was separated into supernatant (100,000 *g*, 1 h), plasma membrane (polyethylene glycol), and endomembrane (dextran T500) fractions. A ZmVPP5-specific antibody was used to detect the presence of ZmVPP5 in different fractions. ZmVPP5 was detected in the endomembrane and plasma membrane fractions. Then, the nuclei and vacuolar membrane fractions were prepared, and ZmVPP5 was detected in both the vacuolar membrane and nuclei fractions (Figure 3). These data confirmed that ZmVPP5 localized to the plasma membrane, vacuolar membrane and nuclei.

Overexpression of *ZmVPP5* reduces salt tolerance in yeast

VPP function can be characterized in a yeast G19 (△*ena1-4*) mutant, which lacks the plasma membrane Na^+ pump and displays salt hypersensitivity (Gao et al. 2006). VPPs can transport H^+ across the vacuolar membrane and enhance Na^+ transport into vacuoles. Therefore, the overexpression of VPP-like proteins can overcome the salt hypersensitivity phenotype of the yeast G19 mutant.

We characterized ZmVPP5 in a yeast G19 mutant strain. The influence of NaCl solution with different concentrations (from 0 mM to 550 mM) was tested for growth of the G19 strain. G19 displayed a salt hypersensitivity phenotype on AP plates with 150-mM and 200-mM NaCl. Compared to G19, the wild-type W303-1A strains grew well on the AP plates with

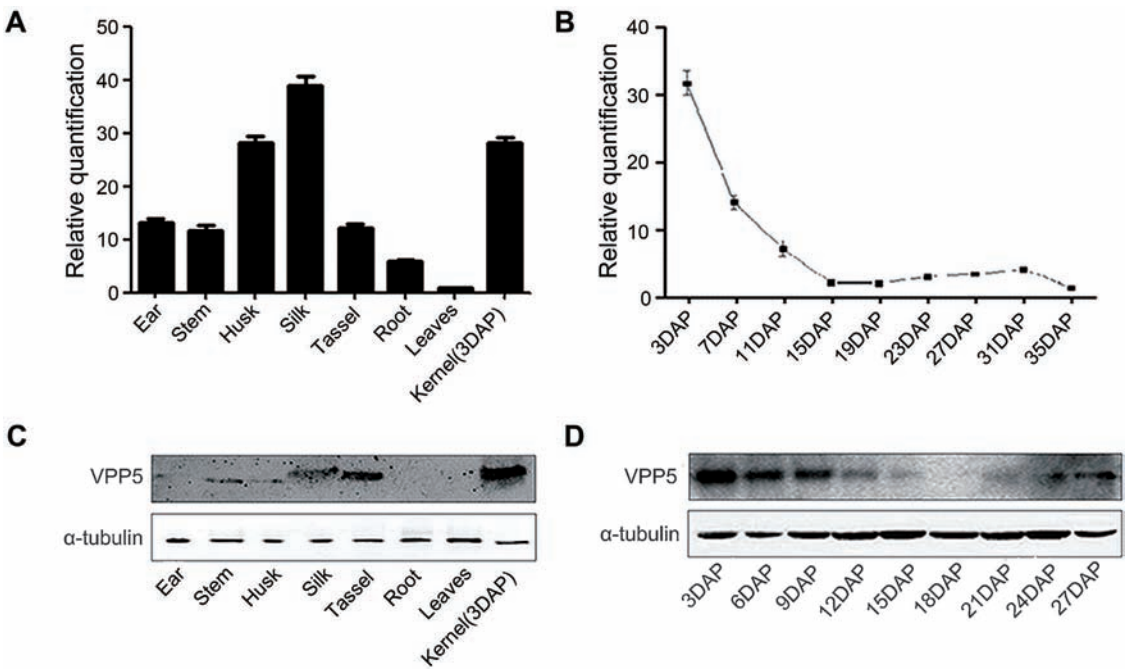

Figure 2. Expression pattern of *ZmVPP5*

(A) Expression profiles of *ZmVPP5* in different tissues. Ubiquitin was used as the internal control. For each RNA sample, three technical replicates were performed. **(B)** Expression profiles of *ZmVPP5* during maize kernel development. **(C)** Western blot analysis of ZmVPP5 in different tissues, α-tubulin was used as a loading control. **(D)** Western blot analysis of ZmVPP5 during maize kernel development.

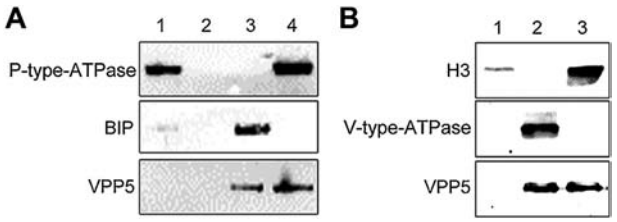

Figure 3. ZmVPP5 is found in the plasma membrane, vacuolar membrane, and nuclei
(A) Detection of ZmVPP5 in the plasma membrane. H^+-ATPase was used as a plasma membrane localization marker, and BIP was used as an ER marker. 1, total protein; 2, supernatant; 3, endomembrane fraction; 4, plasma membrane fraction. **(B)** Detection of ZmVPP5 in the vacuolar membrane fraction and nuclei fraction. Histone 3 was used as a nuclear marker, and V-ATPase was used as a vacuolar membrane marker. 1, total protein; 2, vacuolar membrane fraction; 3, nuclei fraction.

NaCl. At 150-mM NaCl, overexpression of *ZmVPP5* in the G19 mutant strain did not complement the G19 mutant phenotypes but did increase the salt hypersensitivity (Figure 4). These results showed that *ZmVPP5* cannot function as a complete V-PPase in yeast cells. The overexpression of *ZmVPP5* can increase the salt hypersensitivity of the G19 strain. In the wild-type W303-1A strain, the overexpression of *ZmVPP5* also slightly increased the salt hypersensitivity phenotype at 150-mM NaCl (Figure 4), and the phenotype was more apparent at higher NaCl concentrations (450-mM NaCl, Figure S3).

Transgenic maize with overexpressed *ZmVPP5* is more sensitive to high salinity

Transgenic maize overexpressing *ZmVPP5* driven by a double CaMV 35S promoter was successfully generated using Agrobacterium-mediated transformation. Two independent transgenic maize lines were obtained: *35S-VPP5-1(Ox-1)* and *35S-VPP5-2(Ox-2)*. Southern blot analysis showed that *Ox-2* had a single copy of the transgenic fragment and *Ox-1* had 3 copies (Figure 5A). The expression of ZmVPP5 was detected by western blot. The results showed that a high level of ZmVPP5 protein was detected in *OxVPP5* maize (Figure 5B). PCR analysis confirmed the presence of *35S-VPP5* in the transgenic maize and its absence in wild-type maize (Figures 5C, S4).

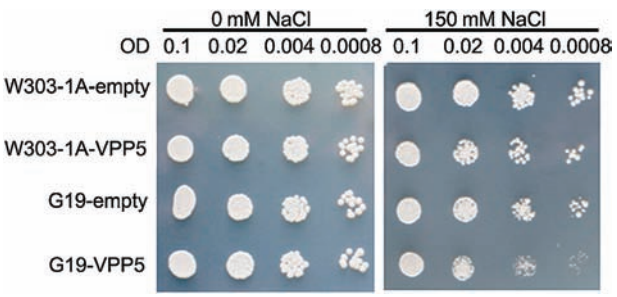

Figure 4. Salt-hypersensitivity assay in G19 and W303-1A yeast
The W303-1A and G19 yeast were transformed with pAJ401 or *pAJ401-ZmVPP5*. Transformations were cultivated on AP plates with 0-mM or 150-mM NaCl for 5 d.

Transgenic *OxVPP5* maize and wild-type maize were grown under normal conditions and under salt stress. After cultivation in 0-mM NaCl for 3 weeks, the height of the wild-type seedlings was similar to that of *OxVPP5*. However, the transgenic maize seedlings of *Ox-1* were significantly smaller than those of wild-type maize in 150-mM and 200-mM NaCl (Figures 5D, S4). The roots length, fresh weight and dry weight of *Ox-2* were also reduced after cultivating in 200-mM NaCl (Figure 5E, F, G). Thus, overexpression of *ZmVPP5* reduced the salt tolerance of the transgenic maize.

The reduced leaf growth under 150-mM and 200-mM salt treatment indicated a reduced salt tolerance in the transgenic *OxVPP5* maize. To determine if other salt stress-responsive genes had corresponding changes in their expression, *ZmSDR, ZmrbcS, ZmPSI-N* and *ZmVPP1* were examined by qRT-PCR. Total RNA of wild-type and *OxVPP5* plants was extracted. The expression of these salt stress-responsive genes in wild-type maize increased under high salt treatment. Overexpressing ZmVPP5 suppressed the expression of these salt stress-responsive genes even without salt treatment. Furthermore, the expression of *ZmSDR* and *ZmrbcS* were further inhibited in *OxVPP5* maize under high salt treatment (Figure 6).

ZmBag6 protein interacts with ZmVPP5 in a yeast two-hybrid analysis

ZmVPP5 protein contains three transmembrane domains and a signal peptide. The full-length *ZmVPP5* was not suitable to be used as bait for the yeast two-hybrid analysis. Therefore, a region of 80–146 aa was cloned and constructed as bait (Figure 7A). The background test indicated that the bait vector *pGBKT7-ZmVPP5* was suitable for a two-hybrid screen.

Approximately 2×10^6 yeast transformants were screened, and 254 putative positive clones were obtained. Sequencing analysis revealed 42 different cDNA sequences. The sequences with results from more than two independent positive clones are listed in Table 1. The full-length clones of these sequences were constructed into the pGBKT7 vector and then co-transformed into AH109 with *pGBKT7-ZmVPP5* to confirm the interaction. The results indicated that ZmBag6 has a stable interaction with the ZmVPP5 fragment in yeast (Figure 7B).

ZmBag6 (NP_001170766) contains a 996 bp open reading frame that encodes a 321 amino acid protein with a calculated molecular weight of 33.5 kDa. Sequence analysis revealed that this sequence encodes a large proline-rich ZmBag6-A-like isoform protein with an unknown function.

ZmBag6 interacts with ZmVPP5 *in vitro* and *in vivo*

To investigate the subcellular localization of ZmVPP5 and ZmBag6, the genes were constructed into the pB7WGY2 and pB7CWG2 vectors. When ZmVPP5 was expressed alone, the signal was detected in the plasma membrane, vacuolar membrane and nuclei (Figure 8A). When ZmBag6 was expressed alone, the signal was found in the nucleus (Figure 8B). Co-expression analysis showed that YFP-ZmVPP5 and CFP-ZmBag6 proteins co-localize in nuclei (Figure 8C).

To examine the interaction between ZmVPP5 and ZmBag6 *in vivo*, a BiLC assay was performed (Zhang et al.

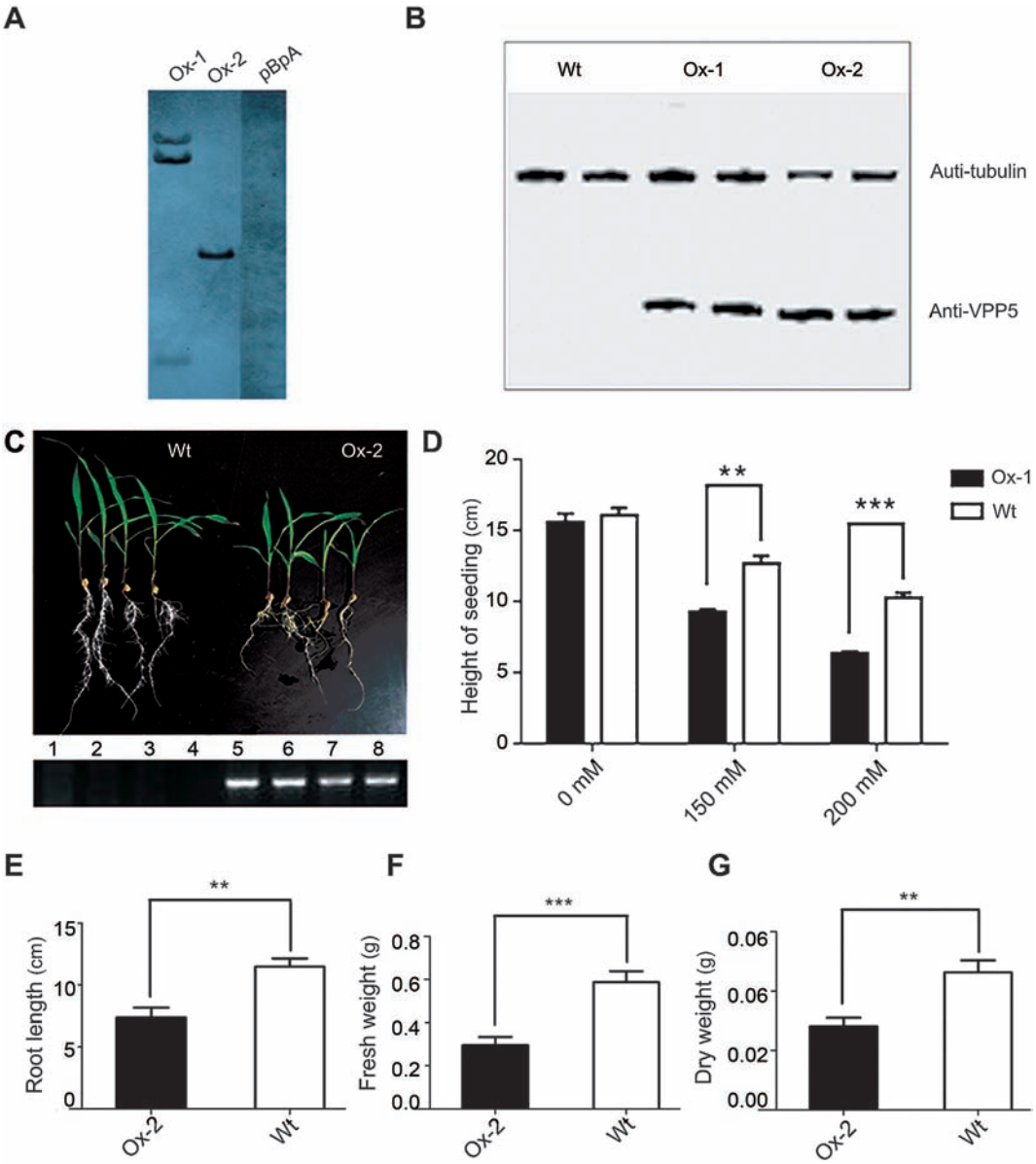

Figure 5. Phenotype analysis of transgenic maize overexpressing *ZmVPP5*

(A) Southern blot analysis of transgenic maize lines *Ox-1* and *Ox-2*. **(B)** Western blot analysis of ZmVPP5 in wild-type and *OxVPP5* maize seedlings. Two protein extracts of each line were loaded and detected. **(C)** Image of wild-type (lanes 1–4) and transgenic maize lines (lanes 5–8) after cultivating in 200 mM NaCl. The lower panel was molecular characterization by PCR with *BAR* gene-specific primers. **(D)** Seedling height of wild-type and transgenic maize lines after cultivating in 0 mM, 150 mM and 200 mM NaCl; Values are the mean values with standard errors, $n = 18$ individuals ($^{**}P < 0.01$, $^{***}P < 0.001$, Student's *t*-test). **(E)** Root length of wild-type and transgenic maize lines after cultivating in 200-mM NaCl; Values are the mean values with standard errors, $n = 12$ individuals ($^{**}P < 0.01$, Student's *t*-test). **(F)** Fresh weight of wild-type and transgenic maize lines after cultivating in 200-mM NaCl; Values are the mean values with standard errors, $n = 12$ individuals ($^{***}P < 0.001$, Student's *t*-test). **(G)** Dry weight of wild-type and transgenic maize lines after cultivating in 200-mM NaCl; values are the mean values with standard errors, $n = 12$ individuals ($^{**}P < 0.01$, Student's *t*-test).

2015b). ZmVPP5 and ZmBag6 were fused to the C- and N-terminal domains of luciferase (CLUC and NLUC). The co-transformation of ZmVPP5-NLUC and ZmBag6-CLUC into an *N. benthamiana* leaf produced strong luciferase activity, while the control had no detectable signal (Figure 9). This result demonstrated that ZmVPP5 can interact with ZmBag6 *in vivo*.

DISCUSSION

We characterized a novel VPP family member, ZmVPP5, which encodes a ZmVPP1-derived protein that lacks several known functional domains. The VPP family proteins play an important role in Pi balance and in the establishment of a proton motive

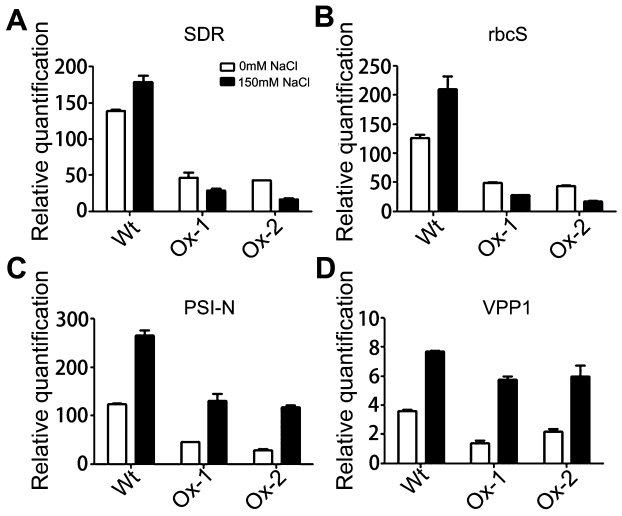

Figure 6. Relative expression of salt stress-responsive genes in wild-type and *OxVPP5* maize seedlings
Total RNA was extracted from 150 mM NaCl-treated and non-treated wild-type and transgenic OxVPP5 plants. The expression levels of **(A)** *ZmSDR*, **(B)** *ZmrbcS*, **(C)** Zm*PSI-N* and **(D)** *ZmVPP1* were analyzed with qRT-PCR. Each column represents an average of three replicates, and bars indicate SDs. Ubiquitin was used as a housekeeping gene.

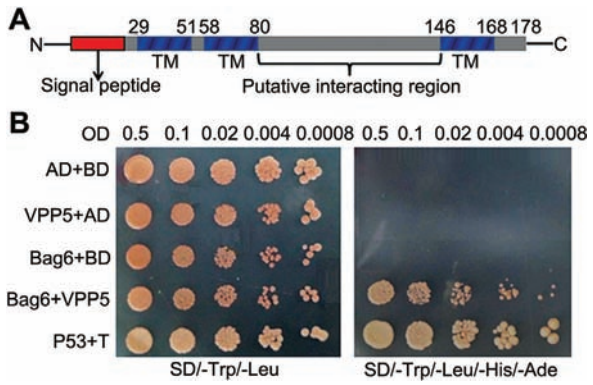

Figure 7. Yeast two-hybrid analyses
(A) ZmVPP5 putative interaction region was constructed into the pGBKT7 vector as the bait vector. **(B)** Yeast two-hybrid interaction analysis between ZmVPP5 and ZmBag6-like protein. AD is the GAL4 activation domain, and BD is the GAL4 DNA binding domain. AD + BD, BD-ZmVPP5 + AD and AD-ZmBag6 + BD are negative controls. P53 + T is a positive control where P53 (murine P53) is fused to BD, and SV40 (large T antigen) is fused to AD. Yeast cells were cultured on selective plates DDO (SD/-Trp/-Leu) and QDO (SD/-Trp/-Leu/-His/-Ade).

force across tonoplasts (Ferjani et al. 2011; Li et al. 2014). Previous studies of V-PPase have mainly focused on the conservative sites and conservative domain structures that are necessary for enzyme activity (Kim et al. 1995; Nakanishi et al. 2001; Van et al. 2005; Asaoka et al. 2014). According to the X-ray crystal structure, the inside of the VPP ion channels is composed of TM5, TM6, TM11, TM12, TM15 and TM16, the combination of which form the catalytic domain containing the motifs for Mg-PPi binding, PPi hydrolysis and energy conversion (Leigh et al. 1992; Nakanishi et al. 2001). Four TMs (TM12-TM15) participate in the dimerization of V-PPase, which primarily involves hydrophobic interactions, six hydrogen bonds and two salt bridges (Lin et al. 2012). ZmVPP5 shares more than 89% protein similarity with TM12-TM15 of ZmVPP1 (Figure S5), but ZmVPP5 does not contain the other known functional domains and key amino acids of V-PPase. ZmVPP5 also has an additional signal peptide (Figure 1). The localization of ZmVPP5 is significantly distinct from type I V-PPase, which might due to the signal peptides and the absence of some functional domains for localization in typical VPPs.

Phylogenetic analysis indicated that ZmVPP5 and other truncated forms of VPPs have an independent origin (Figure S1). These proteins are probably derived from the gene duplication of full-length VPPs. Sharing a similar evolutionary mode with the VPP family, V-ATPase also evolved by gene duplications and sequence divergence, followed by functional and expression pattern changes (Bageshwar et al. 2005; Gaxiola et al. 2007). For example, *Arabidopsis* VHA-B1 and VHA-B3, which are derived from a recent duplication in the *Arabidopsis* genome and are 98% identical, have different functions (Sze et al. 2002; Cho et al. 2006). The truncated H-NS-like protein, lacking the DNA-binding domain of the H-NST family, acts as an H-NS antagonist (Williamson and Free 2005).

VPP family genes have been overexpressed in many species and confer a variety of biological traits, including biomass increase and an increase in stress tolerance (Li et al. 2010; Anjaneyulu et al. 2014). In contrast to full-length VPPs, overexpressing *ZmVPP5* in maize appears to increase the sensitivity to high salinity (Figure 5). Compared with wild-type, *OxVPP5* plants display more wilted leaves and lower seedling height. The expression of the salt stress-responsive genes *ZmSDR*, *ZmrbcS*, *ZmPSI-N* and *ZmVPP1* was also changed in *OxVPP5* transgenic maize (Figure 6). Therefore, *ZmVPP5* might play a role as an inhibitor of salt tolerance. A previous study indicated that TM13–TM15 participate in subunit interactions (Lin et al. 2012). ZmVPP5 may interfere with ZmVPP1 function by heterodimerizing with TM13–TM15.

Members of the VPP family are mainly detected in the plasma membrane, tonoplast, trans Golgi network, and multivesicular bodies (Ratajczak et al. 1999). However, ZmVPP5 was detected in the plasma membrane, vacuolar membrane and the nuclei. ZmVPP5 contains the highly conserved sequence RQFNTIP, which may interact with an important signal protein called 14-3-3 protein. In maize, 14-3-3 protein can be detected after short-term salt stress and is involved in the regulation of the plasma membrane and the vacuole H^+-ATPase that mediates wall acidification in plants (Zorb et al. 2010).

We identified a ZmBag6-like protein that interacted with ZmVPP5 using a yeast two-hybrid screen (Figure 7). ZmBag6 and ZmVPP5 had overlapping sub-cellular localizations in the cell nuclei, and their interaction *in vivo* was confirmed in a BiLC assay (Figure 8). BAG6/BAT3 is a stress-upregulated CaM-binding protein that plays an important role in the suppression

Table 1. Summary of the putative proteins interacting with ZmVPP5 using a yeast two-hybrid assay

Contig[a]	BlastP[b]	Repetitions[c]	Gene annotation[d]
1	NP_001170766	133	Large proline-rich protein ZmBag6-A-like isoform
2	NP_001105988	30	Putative splicing factor
3	NP_001170082	5	Endochitinase A
4	AGF39572.1	3	Kunitz-type protease inhibitor B
5	CAE45949.1	2	2-dehydropantoate 2-reductase
6	AFW89454.1	2	40S ribosomal protein SA
7	AFW62691.1	2	Putative RNA-binding protein

[a]Assembly sequence from the sequencing results of independent positive clones. [b]BlastP results using the protein sequence were confirmed to be in frame with GAL4 protein. [c]The number of independent positive clones homologous to the same gene. [d]Based on BlastX results for the best fit.

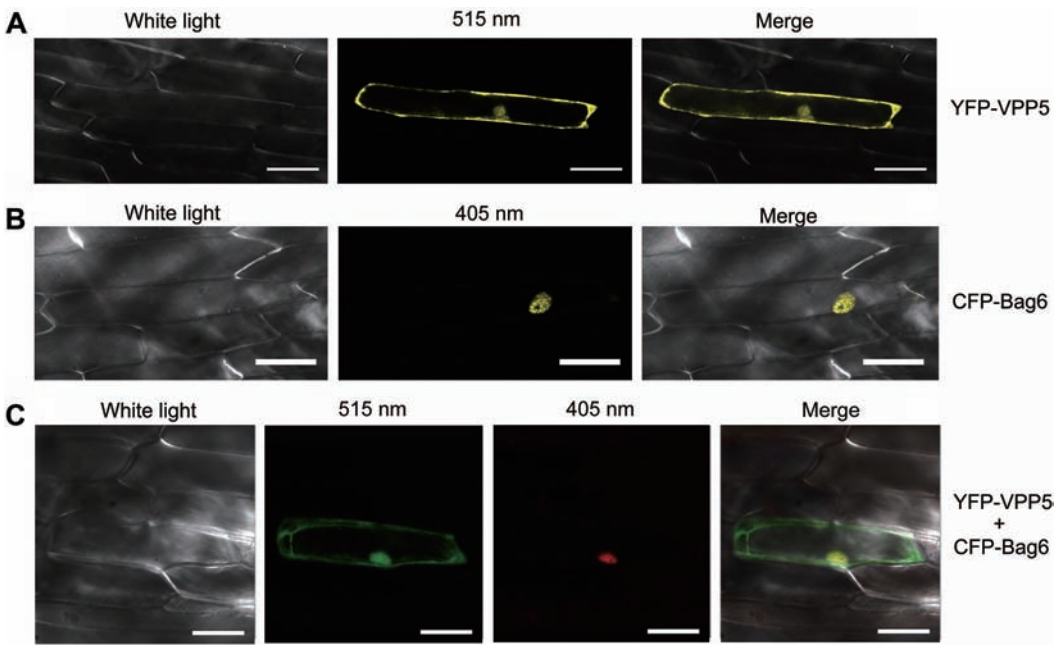

Figure 8. Co-localization of ZmVPP5 and ZmBag6 in onion epidermis
(A) YFP-ZmVPP5 was transiently expressed in onion epidermis. **(B)** CFP-Bag6 was transiently expressed in onion epidermis. **(C)** YFP-ZmVPP5 and CFP-ZmBag6 were co-expressed in onion epidermis. White Bars represent 100 μm.

of NaCl-induced PCD and chromatin regulation (Kang et al. 2006; Krenciute et al. 2013). Bag6 also can inhibit autophagy by affecting the intracellular localization of EP300/p300 (Sebti et al. 2014). Overexpressing *ZmVPP5* might inhibit these processes through ZmVPP5-ZmBag6 interaction and produce a salt hypersensitivity phenotype.

MATERIALS AND METHODS

Plant material

Seeds of the maize (*zea mays*) inbred lines W22, the Hi-II parent A (pA) and the Hi-II parent B (pB) were obtained from the Maize Genetic Cooperation Stock Center and cultivated in the field at Shanghai University, Shanghai, China. F2 Hi-II hybrid (pApB) seeds were derived from a cross between pA and pB. The root, stem, the third leaf, silk, tassel, and ear tissues were collected from at least three W22 plants during male flower powdering. The immature seeds were harvested at 3, 6, 7, 9, 11, 12, 15, 18, 19, 21, 24, 23, 27, 31, and 35 d after pollination (DAP), immediately frozen in liquid nitrogen and stored at −80 °C for RNA and protein extraction.

ZmVPP5 gene cloning

Total RNA was extracted from the maize leaves harvested after two weeks of seed germination using Trizol (TIANGEN, China) reagent. First-strand cDNA was synthesized by the Transcriptor First-Strand cDNA Synthesis Kit (Roche). The cDNA of *ZmVPP5* was obtained by PCR. The primers were designed according to NP_001140455 (Table S1).

Polyclonal antibodies

For anti-ZmVPP5 antibody production, the full-length ZmVPP5 open reading frame (ORF) was amplified, and the PCR products were cloned into the pGEM18-T vector and sequenced. A C-terminal specific polypeptide "VSGVQPSFSLNRKEL" was

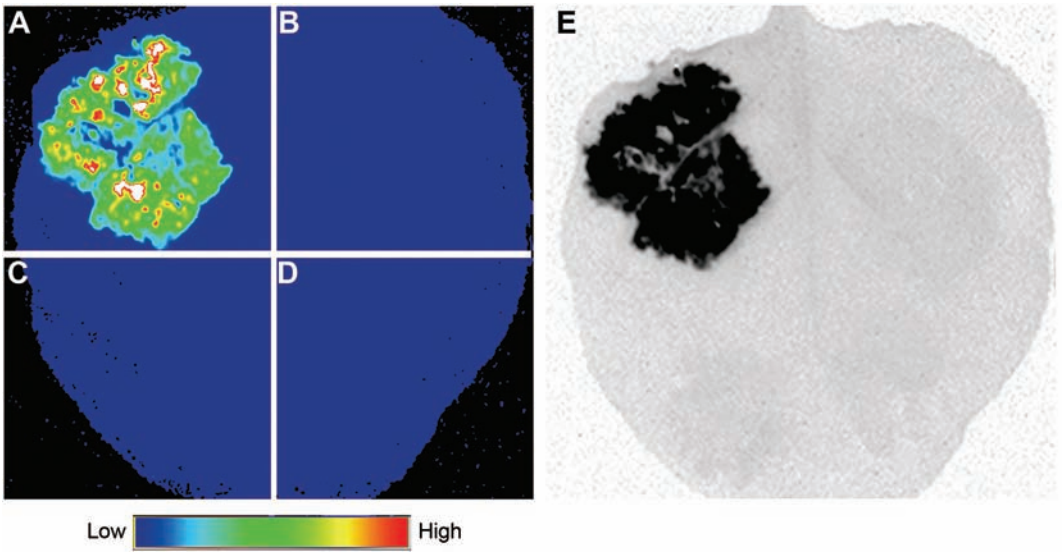

Figure 9. BiLC assay showing that ZmVPP5 interacts with ZmBag6
Bioluminescence signal intensities represent the interaction activities. **(A)** ZmBag6-NLUC+ZmVPP5-CLUC. **(B)** ZmBag6-NLUC+CLUC. **(C)** NLUC+ZmVPP5-CLUC. **(D)** NLUC+CLUC. **(E)** Bright field image as a control.

also used as the antigen. The antibodies were prepared in rabbits using standard protocols by ABclonal Biotechnology Co., Ltd.

Quantitative real-time RT-PCR analysis

Quantitative real-time RT-PCR was performed using a Mastercycler ep realplex 2 (Eppendorf) with SYBR Green Real-Time PCR Master Mix (Toyobo) according to the manufacturer's protocol. Specific primers for ZmVPP5 and ubiquitin were designed online (http://www.quantprime.de/) and are listed in Table S1. The qRT-PCR experiments were performed with two independent sets of RNA samples and three technical replicates. Ubiquitin was used as an internal control (Wang et al. 2012).

Phylogenetic analysis

Homology sequences were identified in the NCBI non-redundant (nr) protein sequences database by a BLASTp search with the ZmVPP5 protein sequence in plants ranging from algae to angiosperms. Then, these sequences were aligned using ClustalW in the MEGA6 package (Tamura et al. 2013). The phylogenetic tree was constructed by the neighbor-joining method, and the evolutionary distances were produced with MEGA6 using bootstrap analysis (1,000 replicates).

Subcellular fractionation and immunoblotting analysis

Plasma membrane vesicles were prepared at 4 °C using the aqueous polymer two-phase partitioning method as described by Wang (Wang et al. 2012) with minor modification. Tonoplast-enriched membrane vesicles were isolated from tassel using differential centrifugation according to a procedure described elsewhere (Rocha Facanha and de Meis 1998). The nuclei were isolated from tassel following a previously described procedure (Folta and Kaufman 2006). The plant compartment marker antibodies, and plasma membrane H^+-ATPase and V-type ATPase antibodies, were obtained from Agrisera (Vännäs, Sweden).

Functional analysis in yeast

The *ZmVPP5* coding region was amplified from the cDNA clone by PCR. After sequencing in pMD18-T, *ZmVPP5* was subcloned into the shuttle vector pAJ401 with *EcoRI* and *XhoI*. Then, the pAJ401 vector was transformed into the yeast salt-hypersensitive mutant G19 (*MATα,leu2-3,tep1-1,ura3-3,ade2-1, his3-11, can1-100,enal△::HIS::Δena4*) and its wild-type W303-1A (*Matα ade2-1 his3-11 15 μra3-1 leu2-3 112trp1*), according to the manufacturer's instructions (Clontech). For the salt tolerance assays, the transformations were cultured in arginine-phosphate (AP) medium (Meng et al. 2011) plus 2% glucose until the OD600 reached 0.5, then 5 μL of fivefold serial dilutions of cell solution was spotted on AP medium supplemented with 0.15 M NaCl at 30 °C for 4 d.

Generation of transgenic maize overexpressing *ZmVPP5*

The entire coding sequence of *ZmVPP5* was amplified from the cDNA clone and ligated between *BamHI* and *HindIII* sites of the pHB vector (Wang et al. 2011), which carries a *BAR (herbicide resistant gene)* resistance marker and a CaMV 35S promoter. PHB-*ZmVPP5* was transformed into the *Agrobacterium tumefaciens* strain EAH105. Agrobacterium-mediated maize transformation using 12 DAP immature zygotic embryos of the Hi-II hybrid (pApB) was carried out according to Frame et al. (2002). PCR, southern blotting and western blotting were used to confirm stable transformation and gene copies (Frame et al. 2002).

Hydroponic cultures and Salt tolerance assay

Maize seeds were surface-sterilized by 3% sodium hypochlorite for 3–5 min, and then germinated at 20 °C for 14 d on moist filter paper in Petri dishes. Individual uniform-size seedlings were transplanted to 2-L plastic boxes for hydroponic culture.

The treatment included control (0 mM NaCl) and NaCl-sufficient salt stress (150 mM and 200 mM NaCl). The plants were cultured in a light incubator at 25–30 °C and a 16 h/8 h light/dark photoperiod. The seedling height was measured after 7 d of culture.

For the salt tolerance assay, the seedlings of the wild-type and OxVPP5 lines were collected and immediately stored in liquid nitrogen. qRT-PCR was performed to analyze the expression of salt stress-responsive genes (Wang et al. 2013), including SDR (short chain dehydrogenase/reductase superfamily, XM_008671320.1), rbcS (Ribulose-1, 5-bisphosphate carboxylase/oxygenase, NM_001152571.1), PSI-N (photosystem I reaction center subunit N, BT034060) and VPP1 (NM_001111910). Tubulin was used as the endogenous reference.

Yeast two-hybrid screening

The yeast two-hybrid library containing a maize seed cDNA library was constructed by Zhang Nan (Zhang et al. 2012). The library contained approximately 1.5×10^6 clones. After culturing, the plasmids were extracted.

The region from 80 to 146 aa of ZmVPP5 was inserted into the pGBKT7 vector. The *pGBKT7-ZmVPP5* was co-transformed into a yeast cell line AH109 with *pGADT7-Recm* using the LiAc method for the background test. Then, the yeast two-hybrid screenings were carried out according to the Yeast Protocols Handbook (BD Biosciences Clontech). The plasmids from all of the positive clones were extracted and amplified in *E. coli*. All of the clones were sequenced and analyzed by GenBank Blastx analysis.

The full-length cDNA of the putative interacting genes that had more than two independently verified clones were amplified for further analysis. The putative positive clones with a full ORF region were then spotted in a dilution series on QDO.

Sub-cellular localization with fluorescent protein fusion

The coding region of *ZmVPP5* and *ZmBag6* was cloned into the gateway entry vector pENTR/D-Topo (pENTR/D-TOPO Cloning Kit, Invitrogen). Then, the entry vectors were recombined with pB7YWG2. CD3-975 and CD3-1007 were bought from tair (http://www.arabidopsis.org/). The living onion epidermal cells were cultured on MS medium in the dark for 8 h. Gene Gun-mediated onion transformation was carried out using the Biolistic PDS-1000/He Gene Gun System (Bio-Rad) (Nagegowda et al. 2005). Bombarded epidermal cells were incubated for 16–24 h at 25 °C in darkness. Confocal imaging was performed using a ZEISS LSM 710 confocal microscope. These experiments were repeated at least three times with similar results.

Bimolecular luminescence complementation assay

Open reading frames of *ZmVPP5* and *ZmBag6* were cloned into JW771 (NLUC) and JW772 (CLUC). Then, these constructs were transformed into *Agrobacterium tumefacien* GV3101. Different combinations of GV3101-VPP5 and GV3101-Bag6 constructs were infiltrated into 5-week-old *Nicotiana benthamiana* leaves using a syringe for BiLC analyses (Zhang et al. 2015a). After growing for 48 h under 16 h of light and 8 h of dark, the leaves were injected with 1 mM luciferin, and the resulting luciferase signals were captured using the Tanon-5200 image system. These experiments were repeated at least three times with similar results.

ACKNOWLEDGEMENTS

This work was supported by the National Natural Sciences Foundation of China (31425019 and 91335208), and the Ministry of Science and Technology of China (2014CB138204).

AUTHOR CONTRIBUTIONS

R.S., W.Q. and X.S. designed the experiment. X.S., Y.Y. and H.L. performed the experiments. X.S., W.Q., G.W. and R.S. analyzed the data. X.S., W.Q. and R.S. wrote the article.

REFERENCES

Anjaneyulu E, Reddy PS, Sunita MS, Kishor PB, Meriga B (2014) Salt tolerance and activity of antioxidative enzymes of transgenic finger millet overexpressing a vacuolar H^+-pyrophosphatase gene (SbVPPase) from Sorghum bicolor. **J Plant Physiol** 171: 789–798

Asaoka M, Segami S, Maeshima M (2014) Identification of the critical residues for the function of vacuolar H^+-pyrophosphatase by mutational analysis based on the 3D structure. **J Biochem** 156: 333–344

Bageshwar UK, Taneja-Bageshwar S, Moharram HM, Binzel ML (2005) Two isoforms of the A subunit of the vacuolar H^+-ATPase in *Lycopersicon esculentum*: Highly similar proteins but divergent patterns of tissue localization. **Planta** 220: 632–643

Cho YH, Yoo SD, Sheen J (2006) Regulatory functions of nuclear hexokinase1 complex in glucose signaling. **Cell** 127: 579–589

Dell'orto M, Nisi PD, Vigani G, Zocchi G (2013) Fe deficiency differentially affects the vacuolar proton pumps in cucumber and soybean roots. **Front Plant Sci** 4: 326

Ferjani A, Segami S, Horiguchi G, Muto Y, Maeshima M, Tsukaya H (2011) Keep an eye on PPi: The vacuolar-type H^+-pyrophosphatase regulates postgerminative development in *Arabidopsis*. **Plant cell** 23: 2895–2908

Folta KM, Kaufman LS (2006) Isolation of *Arabidopsis* nuclei and measurement of gene transcription rates using nuclear run-on assays. **Nat Protoc** 1: 3094–3100

Frame BR, Shou H, Chikwamba RK, Zhang Z, Xiang C, Fonger TM, Pegg SE, Li B, Nettleton DS, Pei D, Wang K (2002) *Agrobacterium tumefaciens*-mediated transformation of maize embryos using a standard binary vector system. **Plant Physiol** 129: 13–22

Gao F, Gao Q, Duan X, Yue G, Yang A, Zhang J (2006) Cloning of an H^+-PPase gene from *Thellungiella halophila* and its heterologous expression to improve tobacco salt tolerance. **J Exp Bot** 57: 3259–3270

Gaxiola RA, Palmgren MG, Schumacher K (2007) Plant proton pumps. **FEBS Lett** 581: 2204–2214

Gaxiola RA, Rao R, Sherman A, Grisafi P, Alper SL, Fink GR (1999) The *Arabidopsis thaliana* proton transporters, AtNhx1 and Avp1, can function in cation detoxification in yeast. **Proc Natl Acad Sci USA** 96: 1480–1485

Jiang L, Phillips TE, Rogers SW, Rogers JC (2000) Biogenesis of the protein storage vacuole crystalloid. **J Cell Biol** 150: 755–770

Kang CH, Jung WY, Kang YH, Kim JY, Kim DG, Jeong JC, Baek DW, Jin JB, Lee JY, Kim MO, Chung WS, Mengiste T, Koiwa H, Kwak SS,

Bahk JD, Lee SY, Nam JS, Yun DJ, Cho MJ (2006) AtBAG6, a novel calmodulin-binding protein, induces programmed cell death in yeast and plants. **Cell Death Differ** 13: 84–95

Kim EJ, Zhen RG, Rea PA (1995) Site-directed mutagenesis of vacuolar H^+-pyrophosphatase. Necessity of Cys^{634} for inhibition by maleimides but not catalysis. **J Biol Chem** 270: 2630–2635

Krenciute G, Liu S, Yucer N, Shi Y, Ortiz P, Liu Q, Kim BJ, Odejimi AO, Leng M, Qin J, Wang Y (2013) Nuclear BAG6-UBL4A-GET4 complex mediates DNA damage signaling and cell death. **J Biol Chem** 288: 20547–20557

Leigh RA, Pope AJ, Jennings IR, Sanders D (1992) Kinetics of the Vacuolar H-Pyrophosphatase: The roles of magnesium, pyrophosphate, and their complexes as substrates, activators, and inhibitors. **Plant Physiol** 100: 1698–1705

Li J, Yang H, Peer WA, Richter G, Blakeslee J, Bandyopadhyay A, Titapiwantakun B, Undurraga S, Khodakovskaya M, Richards EL, Krizek B, Murphy AS, Gilroy S, Gaxiola R (2005) *Arabidopsis* H^+-PPase AVP1 regulates auxin-mediated organ development. **Science** 310: 121–125

Li X, Guo C, Gu J, Duan W, Zhao M, Ma C, Du X, Lu W, Xiao K (2014) Overexpression of VP, a vacuolar H^+-pyrophosphatase gene in wheat (*Triticum aestivum* L.), improves tobacco plant growth under Pi and N deprivation, high salinity, and drought. **J Exp Bot** 65: 683–696

Li Z, Baldwin CM, Hu Q, Liu H, Luo H (2010) Heterologous expression of *Arabidopsis* H^+-pyrophosphatase enhances salt tolerance in transgenic creeping bentgrass (*Agrostis stolonifera* L.). **Plant Cell Environ** 33: 272–289

Lin SM, Tsai JY, Hsiao CD, Huang YT, Chiu CL, Liu MH, Tung JY, Liu TH, Pan RL, Sun YJ (2012) Crystal structure of a membrane-embedded H^+-translocating pyrophosphatase. **Nature** 484: 399–403

Maeshima M (2000) Vacuolar H^+-pyrophosphatase. **Biochim Biophys Acta** 1465: 37–51

Meng X, Xu Z, Song R (2011) Molecular cloning and characterization of a vacuolar H^+-pyrophosphatase from Dunaliella viridis. **Mol Biol Rep** 38: 3375–3382

Mitsuda N, Enami K, Nakata M, Takeyasu K, Sato MH (2001) Novel type *Arabidopsis thaliana* H^+-PPase is localized to the Golgi apparatus. **FEBS Lett** 488: 29–33

Mohammed SA, Nishio S, Takahashi H, Shiratake K, Ikeda H, Kanahama K, Kanayama Y (2012) Role of Vacuolar H^+-inorganic pyrophosphatase in tomato fruit development. **J Exp Bot** 63: 5613–5621

Nagegowda DA, Ramalingam S, Hemmerlin A, Bach TJ, Chye ML (2005) *Brassica juncea* HMG-CoA synthase: Localization of mRNA and protein. **Planta** 221: 844–856

Nakanishi Y, Saijo T, Wada Y, Maeshima M (2001) Mutagenic analysis of functional residues in putative substrate-binding site and acidic domains of vacuolar H^+-pyrophosphatase. **J Biol Chem** 276: 7654–7660

Perez-Castineira JR, Hernandez A, Drake R, Serrano A (2011) A plant proton-pumping inorganic pyrophosphatase functionally complements the vacuolar ATPase transport activity and confers bafilomycin resistance in yeast. **Biochem J** 437: 269–278

Ratajczak R, Hinz G, Robinson DG (1999) Localization of pyrophosphatase in membranes of cauliflower inflorescence cells. **Planta** 208: 205–211

Rocha Facanha A, de Meis L (1998) Reversibility of H^+-ATPase and H^+-pyrophosphatase in tonoplast vesicles from maize coleoptiles and seeds. **Plant Physiol** 116: 1487–1495

Sebti S, Prebois C, Perez-Gracia E, Bauvy C, Desmots F, Pirot N, Gongora C, Bach AS, Hubberstey AV, Palissot V, Berchem G, Codogno P, Linares LK, Liaudet-Coopman E, Pattingre S (2014) BAG6/BAT3 modulates autophagy by affecting EP300/p300 intracellular localization. **Autophagy** 10: 1341–1342

Seidel T, Siek M, Marg B, Dietz KJ (2013) Energization of vacuolar transport in plant cells and its significance under stress. **Int Rev Cell Mol Biol** 304: 57–131

Sze H, Schumacher K, Muller ML, Padmanaban S, Taiz L (2002) A simple nomenclature for a complex proton pump: VHA genes encode the vacuolar H^+-ATPase. **Trends Plant Sci** 7: 157–161

Tamura K, Stecher G, Peterson D, Filipski A, Kumar S (2013) MEG A6: Molecular Evolutionary Genetics Analysis version 6.0. **Mol Biol Evol** 30: 2725–2729

Van RC, Pan YJ, Hsu SH, Huang YT, Hsiao YY, Pan RL (2005) Role of transmembrane segment 5 of the plant vacuolar H^+-pyrophosphatase. **Biochim Biophys Acta** 1709: 84–94

van Schalkwyk DA, Saliba KJ, Biagini GA, Bray PG, Kirk K (2013) Loss of pH control in *Plasmodium falciparum* parasites subjected to oxidative stress. **PLoS ONE** 8: e58933

Viotti C, Kruger F, Krebs M, Neubert C, Fink F, Lupanga U, Scheuring D, Boutte Y, Frescatada-Rosa M, Wolfenstetter S, Sauer N, Hillmer S, Grebe M, Schumacher K (2013) The endoplasmic reticulum is the main membrane source for biogenesis of the lytic vacuole in *Arabidopsis*. **Plant Cell** 25: 3434–3449

Wang G, Sun X, Wang G, Wang F, Gao Q, Sun X, Tang Y, Chang C, Lai J, Zhu L, Xu Z, Song R (2011) Opaque7 encodes an acyl-activating enzyme-like protein that affects storage protein synthesis in maize endosperm. **Genetics** 189: 1281–1295

Wang G, Wang F, Wang G, Wang F, Zhang X, Zhong M, Zhang J, Lin D, Tang Y, Xu Z, Song R (2012) Opaque1 encodes a myosin XI motor protein that is required for endoplasmic reticulum motility and protein body formation in maize endosperm. **Plant Cell** 24: 3447–3462

Wang M, Liu C, Li S, Zhu D, Zhao Q, Yu J (2013) Improved nutritive quality and salt resistance in transgenic maize by simultaneously overexpression of a natural lysine-rich protein gene, SBgLR, and an ERF transcription factor gene, TSRF1. **Int J Mol Sci** 14: 9459–9474

Williamson HS, Free A (2005) A truncated H-NS-like protein from enteropathogenic *Escherichia coli* acts as an H-NS antagonist. **Mol Microbiol** 55: 808–827

Zhang N, Qiao Z, Liang Z, Mei B, Xu Z, Song R (2012) *Zea mays* Taxilin protein negatively regulates opaque-2 transcriptional activity by causing a change in its sub-cellular distribution. **PLoS ONE** 7: e43822

Zhang TQ, Lian H, Tang H, Dolezal K, Zhou CM, Yu S, Chen JH, Chen Q, Liu H, Ljung K, Wang JW (2015a) An intrinsic microRNA timer regulates progressive decline in shoot regenerative capacity in plants. **Plant Cell** 27: 349–360

Zhang Z, Yang J, Wu Y (2015b) Transcriptional regulation of Zein gene expression in maize through the additive and synergistic action of opaque2, prolamine-box binding factor, and O_2 heterodimerizing proteins. **Plant Cell** 27: 1162–1172

Zhou Y, Pan X, Qu H, Underhill SJ (2014) Tonoplast lipid composition and proton pump of pineapple fruit during low-temperature storage and blackheart development. **J Membr Biol** 247: 429–439

Zorb C, Schmitt S, Muhling KH (2010) Proteomic changes in maize roots after short-term adjustment to saline growth conditions. **Proteomics** 10: 4441–444

SUPPORTING INFORMATION

Additional supporting information may be found in the online version of this article at the publisher's web-site.

Figure S1. Phylogenetic analysis of plant VPPs

Maize ZmVPP5 and identified VPPs in other plants from algae to angiosperms were aligned using ClustalW. The phylogenetic tree was constructed using MEGA 6.0, and *Scenedesmus vacuolatus* VPP was used as the out-group. Some truncated proteins in different organisms were marked with asterisks.

Figure S2. Subcellular localization of ZmVPP5 in onion epidermal cells and tobacco mesophyll cells

(A) Co-localization of YFP-VPP5 and CD3-975 in onion epidermal cells. **(B)** Co-localization of YFP-VPP5 and CD3-1007 in the case of plasmolysis in onion epidermal cells; CD3-1007 (pm-rk, plasma membrane localization marker, mcherry fluorescent), CD3-975 (vac-rk, vacuole localization marker, mcherry fluorescent). White Bars represent 20 μm.

Figure S3. Salt-hypersensitive assay in W303-1A with *ZmVPP5*

The W303-1A was transformed with pAJ401 or *pAJ401-ZmVPP5*. Transformed cells were cultivated on AP plates with 0 mM or 450 mM NaCl for 5 days.

Figure S4. Phenotypic and molecular characterization of transgenic maize overexpressing ZmVPP5

(A) Image of transgenic maize lines overexpressing *ZmVPP5* and wild-type maize cultivating in 0-mM (lanes 1–6), 150 mM (lanes 7–12) and 200 mM (lanes 13–18) NaCl. **(B)** Image of transgenic maize lines overexpressing *ZmVPP5* and wild-type maize after cultivating in 0 mM (lanes 1–6), 150 mM (lanes 7–12) and 200 mM (lanes 13-18) NaCl.

Figure S5. Sequence alignment of five typical proteins of the VPP subgroups

ClustalW alignment of five typical proteins of the VPP subgroups. The black shading within the white lettering indicates residues conserved in all five members, Type I (NP_001152459), Type II (NP 001105380), Type III (NP 001106067), Type IV (XP 008666607), Type V (VPP5, NP 001140455).

Table S1. Primers used in this study Specific primers for qPCR were designed online (http://www.quantprime.de/), and the other primers were designed using the Primer 5.0 software. F means forward primer. R means reverse primer.